NASA TT F-11,258

THE DETERMINATION OF THE THERMODYNAMIC STATE OF RELAXING HYPERSONIC GAS FLOWS BY ELECTRON COLLISION EXCITATION

K. Bütefisch

Translation of "Die Bestimmung des thermodynamischen Zustandes relaxierender hypersonischer Gasströmungen durch Elektronenstossanregung". Aerodynamische Versuchsanstalt Göttingen (West Germany), DLR-FB-66-63, September 1966, 40 pp.

NATIONAL AERONAUTICS AND SPACE ADMINISTRATION
WASHINGTON, D.C. 20546 OCTOBER 1967

TABLE OF CONTENTS

Designations

d^3r = space element [cm^3]

dn'_e = electron surface density [$cm^{-2}sec^{-1}$]

e = energy of an excited state [erg]

e_o = elementary charge [A sec]

$f(T_v)$ = transfer function for vibrational energy

h = Planck's constant [erg sec]

k = Boltzmann constant [$erg°K^{-1}$]

l_1, l_0 = number of excited and nonexcited molecules, respectively [cm^{-3}]

m_o = electron mass [g]

m, n, n' = vibrational quantum numbers

n_e, n_{eo} = number of electrons [cm^{-3}]

x_o = molecular constant

E = energy [erg]

$G_o(n')$ = wave number of the transition 0, n' [cm^{-1}]

J = intensity

$J(K', T_R)$ = intensity of the rotational lines

$J_{el}(\vartheta)$ = differential scattering cross section for elastic scattering [cm^2]

$J_u(\vartheta)$ = differential scattering cross section for inelastic scattering [cm^2]

K', K'' = rotational quantum numbers

M_1, M_2 = molecular masses

N = number of molecules [cm^{-3}]

$Q_{el}(E)$ = total scattering cross section for elastic scattering [cm^2]

$Q_u(E)$ = total scattering cross section for inelastic scattering [cm^2]

R = gas constant

$|R_{nm}|$ = matrix element of the vibrational transition n, m

T_o = static temperature [°K]

T_{SK} = temperature of black-body emitter [°K]

Z = collision number [sec^{-1}]

$\eta(T)$ = gas viscosity [poise]

ϑ = scattering angle [°]

ν_{nm} = wave number of the transition n, m

σ^2 = collision cross section [cm^2]

φ = azimuthal angle [°]

ψ_v^n, ψ_v^m = wave function for molecular vibrations

ω_o = molecular constant [cm^{-1}]

Λ = orbital angular momentum quantum number

Θ = characteristic temperature [°K]

Subscripts

R = rotation

T = translation

V = vibration

nm, nn' = transition nm or nn', respectively

n, n' = transition in state n or n', respectively

THE DETERMINATION OF THE THERMODYNAMIC STATE OF RELAXING HYPERSONIC GAS FLOWS BY ELECTRON COLLISION EXCITATION

K. Bütefisch

ABSTRACT. In order to determine the thermodynamic state of relaxing hypersonic gas flows, besides the static temperature and density, the vibrational temperature must also be measured. After discussing several possible measurement procedures, a method for determining the vibrational temperature with the aid of the electron collision excitation technique via spectroscopy is described. The special arrangement of the equipment makes it possible to seek continuously and simultaneously, besides the local vibrational temperature also the local density as a function of position or for a given position as a function of total pressure or stagnation temperature.

1. Introduction /8*

In order to describe the flow conditions in a hypersonic wind tunnel, it is necessary to know the thermodynamic state of the test gas. As long as the gas expands isentropically in the nozzle, the Mach number and Reynolds number distributions can be calculated from the measured values for static pressure, static temperature, and Pitot pressure.

If the thermodynamic equilibrium in the expansion flow is not given, then in order to calculate the *Ma* and *Re* distributions in the strip of flow which is to be measured, in addition to Pitot pressure, either static temperature, static pressure or vibrational temperature must also be known. Then it is assumed that from a certain point in the nozzle, the vibrational temperature is frozen in, that is, the vibrational temperature up to the freezing-in point is in equilibrium with the translational and rotational temperatures [1]. After this freezing-in point, the number of molecular collisions is no longer sufficient for energy exchange and the vibrational temperature remains constant. Calculations in which freezing-in is considered as a parameter by way of the freezing-in temperature have been carried out by I. E. Vas and G. Koppenwallner [2] among others. Naturally they require experimental confirmation, which depends on an experimental determination of the vibrational temperature.

In the present report, various methods for determining the vibrational temperature will be studied with respect to their applicability in the hypersonic wind tunnel at low gas densities at the AVA at Göttingen. Because of its good spatial resolution and precision, the electron beam procedure was selected

*Numbers in the margin indicate pagination in the foreign text.

N.B.: Commas should be interpreted as decimal points in all material that has been reproduced directly from the original foreign document.

and described in detail. After the theoretical foundations based on reports by Muntz [3] and Herzberg [4], a description of the measuring apparatus is given, followed by a brief survey of the measurement protocol.

2. Various Methods for Determining the Vibrational Temperatures /9

2.1 Enthalpy in the Case of Diatomic Gases

In the case of a diatomic gas, the total enthalpy $h_o(T)$ is increased by exciting the vibrational and rotational states. Then we have

$$h_o(T) = RT + e_T + e_R + e_V + \frac{\rho}{2} v^2 \quad . \tag{1}$$

R = gas constant, e_T = translational energy, e_R = rotational energy, e_V = vibrational energy, ρ = gas density, and v = gas velocity.

The translational and rotational energies can be replaced by $e_T = 3/2\ RT_T$ and $e_R = RT_R$, where T_T and T_R are the translational and rotational temperatures, respectively. Both temperatures are very low in the expansion flow and are equal to the static temperature T. By means of the relaxation process, a high vibrational temperature is maintained in the expansion flow. If the vibration of a diatomic molecule is described by a harmonic oscillator, the vibrational energy can be expressed [5] by

$$E_V(T_V) = \frac{R\Theta}{e^{\Theta/T_V} - 1} \tag{2}$$

The symbol θ signifies a characteristic temperature and has the value $\Theta = 3{,}374°K$ for N_2.

Since the total enthalpy $h_o(T_o)$ at static temperature T_o is known before the expansion, then from

$$h_o(T_o) = h_o(T, T_V) = \frac{7}{2} RT + \frac{\rho}{2} v^2 + \frac{R\Theta}{e^{\Theta/T_V} - 1} \tag{3}$$

the vibrational temperature T_V can be found. This type of measurement of the /10 vibrational temperature was developed by G. Koppenwallner [6]. The temperature increase of a specified amount of water which was heated by the gas flow was measured using a probe.

2.2 Spectral Reversal Method

The most basic difference between macroscopic measurement using the total enthalpy probe and the microscopic procedure which we are about to describe is that as probes, this latter procedure uses molecules, electrons or quanta of radiation which are permitted to interact directly with the test gas molecules. Thus, the gas-kinetic state of the flow is not disturbed. This is of particularly great advantage in the measurement of models. However, a very good spatial resolution is also required, since despite the stationary operation of the wind tunnel, uniform temperatures cannot be expected over the flow cross section. Boundary layers form in the area close to the walls, and the models which are inserted into the flow stream change the temperature distribution in their own manner.

The best-known procedure for determining the temperature of the gas depends on the fact that many metal atoms can be brought into an electrically excited state by collisions of the second kind. Thus, for example, if small amounts of sodium are added to a gas with temperature T, and if a black-body emitter with the known temperature T_{SK} is observed through the gas, the position of the Na-D lines appears either dark or light in its spectrum, depending on whether T is smaller or larger than T_{SK}. If the two temperatures are the same, the unknown gas temperature T is found by determining this reversal point.

The gas temperature T is defined by the ratio of l_1 excited to l_o non-excited Na atoms [7]:

$$\frac{l_1}{l_o} = \frac{g_1}{g_o} e^{-e/kT} \tag{4}$$

in which a Boltzmann distribution is assumed. Thus, g_1 and g_o are statistical /11 weighting factors, e is the energy of the excited state, and k is the Boltzmann constant.

As more precise investigations have shown, the excited states of the Na atom are populated by interaction with the vibrational states of the N_2 molecules and depopulated by collision processes and radiation.

If Z is the number of possible collisions of an Na atom with N molecules of N_2, l_o is the number of sodium atoms, and $f(T_V)$ is a function which depends only on T_V, which describes the possible transfer of the vibrational energy of the N_2 molecule to the Na atom, then $Z \times f(T_V) \times l_o$ sodium atoms become excited. Thus, in equilibrium, l_1 excited Na atoms are present, so that $Z \times l_1$ sodium atoms revert to the ground state by collisions with N_2 molecules and $A \times l_1$ sodium atoms by spontaneous emission. Thus, the equation for the equilibrium state is as follows:

$$Z \cdot f(T_V) \cdot I_o = Z \cdot I_1 + A \cdot I_1 \quad . \tag{5}$$

The quantity Z can be expressed by the collision formula [8] from gas kinetics:

$$Z = 2 \cdot N \cdot \sigma_{12}^2 \sqrt{2\pi \, RT \, \frac{M_1 + M_2}{M_1 \cdot M_2}} \quad [\sec^{-1}] \quad , \tag{6}$$

where N is the number of N_2 molecules, σ_{12}^2 is the collision cross section, M_1 and M_2 are the masses of the pair involved in the collision, and T is the static temperature. Under normal conditions, Z assumes the value of 8.3×10^9 $\sec^{-1}$, using data from [8]. The quantity A is given by the reciprocal of the life of the excited atom and has the value of 6.3×10^7 $\sec^{-1}$ [8].

From (5) we obtain

$$\frac{I_1}{I_o} = \frac{f(T_V)}{1 + A/Z} \quad . \tag{7}$$

If a and b represent the factors by which N and T deviate from the normal conditions, then Z can be expressed by

$$Z = 8{,}3 \cdot 10^9 \cdot a \cdot \sqrt{b} \quad [\sec^{-1}] \tag{8}$$

/12

Then, inserting the numerical values for A and (8), equation (7) becomes

$$\frac{I_1}{I_o} = \frac{f(T_V)}{1 + 7{,}6 \cdot 10^{-3}/a\sqrt{b}} \tag{9}$$

As long as

$$7{,}6 \cdot 10^{-3}/a\sqrt{b} \ll 1 \tag{10}$$

the ratio I_1/I_o depends only on $f(T_V)$ and thus, on the vibrational temperature. A temperature determination can be carried out by means of equation (4). In the hypersonic wind tunnel, $b \approx 50/273$ and $a \approx 7.6 \times 10^{-3}$, so that this condition (10) can no longer be fulfilled. Then the ratio I_1/I_o also depends on the

density and the static temperature, so that the vibrational temperature can no longer be determined in a simple manner from (4).

The foregoing consideration represents only a rough model. In reality, absorption- and radiation-less transitions must also be taken into consideration. To be sure, these effects become less significant when the pressure is lowered, but it is exactly then when the deviation from the true temperature T_V becomes large.

Hurle *et al.* [5] used this method to study an expansion flow in a 15° nozzle behind a collision wall. The static pressure at the measuring point amounted to *ca.* 73 Torr, so that a small temperature error had to be accounted for. Because they measured the emission ε and the absorption α simultaneously, from the ratio α/ε and the known temperature T_{SK} of the black body, according to the formula

$$\exp\ (-c_2/\lambda T_V) = \frac{1}{1 + \alpha/\varepsilon} \exp\ (-c_2/\lambda T_{SK}),$$

they were able to determine T_V. The volume taken into account in this determination of temperature thus consisted of two spheres formed from a ray bundle /13 focused in the middle of the nozzle (Figure 1a). This ray bundle is used for the most varied temperature ranges with the setup in question, so that the spatial resolution is conceivably quite poor. In any case, it is not sufficient for determining such things as temperature distribution on models.

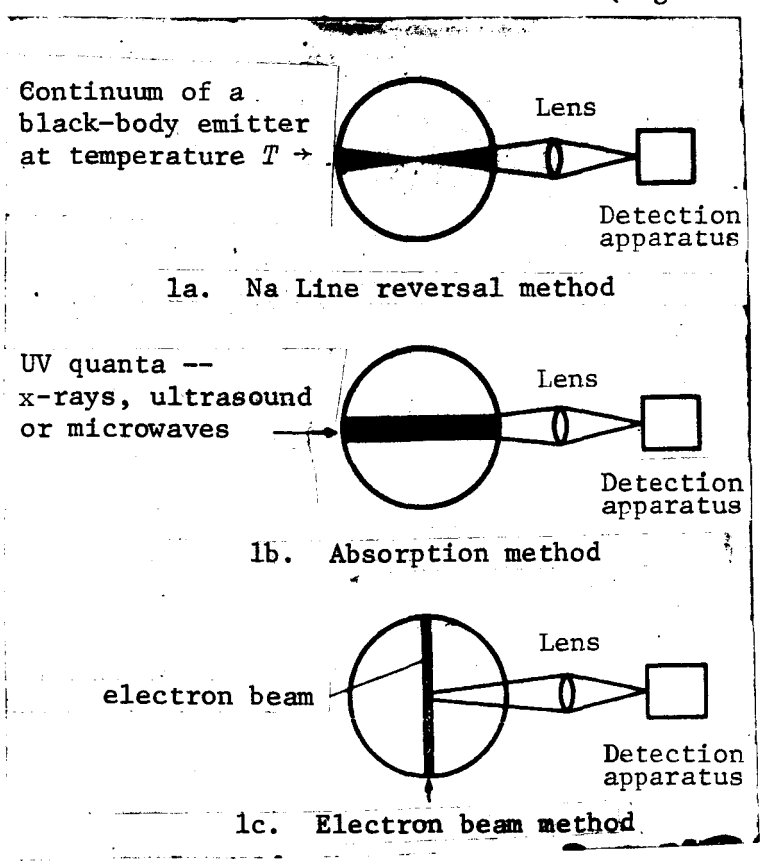

1a. Na Line reversal method

1b. Absorption method

1c. Electron beam method

Figure 1. Spatial Resolution Using Various Methods for Temperature Determination.

2.3 Ultraviolet Absorption Method

In this method, ultraviolet light is passed through the test gas and the absorption is measured [9]. By calibration, the dependence on pressure can be eliminated, so that the absorption is finally a function only of the vibrational temperature. The absorption coefficient is then proportional to the overlap integral

$$\left[\int \psi_v^n \psi_v^m \, d^3 r\right]^2 \quad (11)$$

of the various effective vibrational transitions n, m, whose values increase with increasing quantum numbers n, m. The higher the vibrational temperature is, the more the overlap integrals provide an effective contribution to the absorption coefficient.

In the case of N_2, appreciable absorption only takes place for $\lambda < 800$ Å, so that absorption measurements must be made in vacuum spectrographs, since the oxygen in the air has a powerful absorption capability even below 1,800 Å. The volume to be studied is formed by a cylinder situated transverse to the axis of the wind tunnel, as is shown in Figure 1b. The spatial resolution is once more rather unfavorable, since once again the boundary layers are also included. In addition, the elimination of the density distribution over the tunnel cross section may be a problem. Under certain circumstances, the greater density of the boundary layers may have the same effect at lower temperatures as the slighter density of the nuclear flow, although at higher temperatures. Finally, if we wish to investigate models, then density and temperature once more vary, so that the interpretation of the measured results is also difficult in this case. In principle, absorption measurements can also be carried out with x-rays, ultrasonic or microwave, and the vibrational temperature may also be found in this manner.

Although in these cases certain difficulties can be eliminated by perform- /14
ing measurements in the far ultraviolet, no significant advantages can be expected. The volume to be measured is still in the form of a cylinder, as is represented in Figure 1b.

2.4 Raman Spectroscopy

Whereas the first two methods depend on an effect which is characterized by the overall vibrational state, Raman spectroscopy directly provides the intensity of the individual optical vibrational lines, and the vibrational temperature can be found directly from their distribution. The vibrational spectrum, which lies in the ultrared by virtue of its energy, appears in this case as the satellite spectrum of a single, intensive, incident line in the visible region. The monoenergetic light quanta passed through the test gas lose discrete amounts of energy to the molecules, and these amounts of energy correspond to the vibrational transitions. Since in this case we are dealing with an inelastic scattering process whose cross section is not very large even for large densities of the substance, the application of this method to the small densities in the measuring area of a hypersonic wind tunnel with small gas densities is very problematic. For example, Pohl [10] gives a Raman spectrogram of 0_2 which was taken at a gas pressure of 10 atm with 50 hours illumination time. However, the effect is proportional to the square of the intensity of the incident light, so that an increase in intensity, such as would be possible by using a laser as a light source, might provide better results. A cylinder, as is shown in Figure 1b, would once more be the measuring volume, so that similar difficulties would be inherent in the temperature measurements as in the case of the methods described previously.

2.5 Ionization Method

As long as the gas is in thermal equilibrium, the degree of ionization represents a measure of the gas temperature. However, this effect can only be measured if the temperature is a few 1,000°K. Since no thermal equilibrium can be expected in the expansion flow, and also since the static temperature rapidly drops below 1,000°K, this type of measurement is not possible. /15

As for other procedures, according to a suggestion made by Koppenwallner, one could introduce electrons with defined energies into the test gas and measure the ionization flow in dependence on the electron energy. According to the Frank-Condon principle, it is to be expected that the output energy [11] would possess a fine structure characterized by the vibrational state. Similar results could be given by the electron collision experiment according to Frank-Hertz, in which a fine structure likewise dependent upon the vibrational state could be used for determining the temperature.

For application in a wind tunnel, considerable difficulties would appear in the slight degree of monochromaticity and the large scattering cross section of the low-energy electrons, which could make the application of this method impossible. In addition, the high velocities would disturb the test gas molecules, which would make the determination of energy very difficult.

2.6 Electron Beam Method

Detailed investigations by Muntz [3] have shown that the vibrational temperature can be easily obtained from the spectrum of N_2 molecules excited by electron collision. We shall treat the details of this occurrence very thoroughly in the final section.

The volume for measurement can be made extremely small and far inside the strip to be measured, since the electron beam is passed through the measured strip and an arbitrary portion of the excited area can be focused on a spectrograph and thus analyzed. In this case, the volume which is measured amounts to only a few mm^3 (Figure 1c). Since the light emerging from the excited area is not absorbed by the other molecules, no disturbances due to collisions or boundary layers are to be feared. This procedure offers the possibility of carrying out undisturbed temperature measurements.

3. Critical Comparison of the Various Methods /16

The various methods will be compared with respect to their applicability in the hypersonic wind tunnel at low gas densities.

The low gas density in the strip to be measured makes the application of the line-reversal method impossible, since the population of the excited state, which is dependent on the vibrational temperature, is greatly reduced by natural radiation. Corrections would require a precise knowledge of the static

pressure, which is difficult because of the nonequilibrium expansion flow, and is not possible at all in measurements on models.

The various absorption methods lose a great deal of sensitivity at the low gas pressures, although these difficulties can be compensated for under certain circumstances by suitable detection methods.

Raman spectroscopy is evidently impossible at these low densities, as long as we use the customary light sources. The application of a laser is very expensive.

All of the methods previously mentioned have poor spatial resolution according to Figures 1a and 1b. The volume which is measured includes fractions of the volume which belong to the boundary layer, to the center of flow, or to both, and the measured temperature can only be determined as the mean temperature of the overall volume. As long as the flow conditions are simple, weighing factors can be ascribed to each of the volume fractions, so that the measured temperature can finally be attributed to a smaller volume. But if the flow conditions are complex, as would be expected if models were introduced, this method is not possible. The precision of the temperature determination is not great in any case. Those methods mentioned which depend on ionization effects do provide better spatial resolution, but the difficulties inherent in control of the low-energy electrons and ions are so great that this method is also not applicable in the hypersonic wind tunnel.

The disadvantages which accompany all the methods just described are absent in the case of the electron beam method. The electrons have sufficiently great energy, so that the scattering cross section can be sufficiently small for elastic and inelastic scattering. The slight density in the area to be measured can be compensated for by choosing a larger beam area. The temperature can be attributed to a defined point in space, so that measurements on models become possible [12]. As we will see later, in addition to the local vibrational temperature, we can also measure the local rotational temperature and the local test gas density. For these reasons, the electron beam method was selected for the AVA hypersonic wind tunnel with small gas densities. In the following, this method will be described in greater detail. /17

4. The Theory of the Electron Beam Method

In his reports, Muntz [3] laid all the essential foundations for the application of the electron beam technique. He placed particular emphasis on investigating the usefulness of the electron beam for density determinations [13].

4.1 Elastic Scattering

When electrons of sufficient energy are shot into a gas, they interact in various ways with the gas molecules. First, they can be elastically scattered, *i.e.*, they lose amounts of energy which are small in comparison with $(m_o/M)E$, where m_o is the electron mass, M is the mass of the molecule, and E is the

energy of the primary electron [13].

If electrons moving in the y direction in accordance with Figure 2 are considered, then the number $dn'_e(\vartheta)$ of electrons rotated through the angle ϑ per second and per cm^2 for all azimuthal angles φ is

$$dn'_e(\vartheta) = 2\pi v_e \sin\vartheta \cdot d\vartheta \cdot N \cdot n_e \cdot J_{el}(\vartheta)\, dy \quad , \tag{12}$$

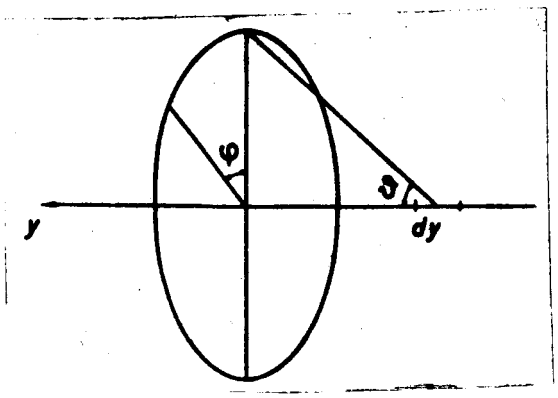

Figure 2. Definition of the Coordinates in Determination of the Scattering Cross Section.

where v_e is the electron velocity, N is the molecular density per cm^3, $J_{el}(\vartheta)$ is /18 the differential scattering cross section for elastic scattering, and dy is the path element. $J_{el}(\vartheta)$ was calculated by Muntz and Marsden [13], using the approximation of Mott and Massey for N, and is plotted in Figure 3 versus the scattering angle ϑ. We see that $J_{el}(0)$ for $\vartheta = 0$ is independent of the energy and has the value of $7.5 \times 10^{-15} cm^2$. For angle $\vartheta > 0$, $J_{el}(\vartheta)$ becomes smaller and, for a fixed angle, diminishes with the square of the energy. The overall effective cross section for elastic scattering is obtained by integration over all

$$Q_{el}(E) = 2\pi \int_0^{\infty} J_{el}(\vartheta) \sin\vartheta\, d\vartheta \tag{13}$$

and is a function of the energy.

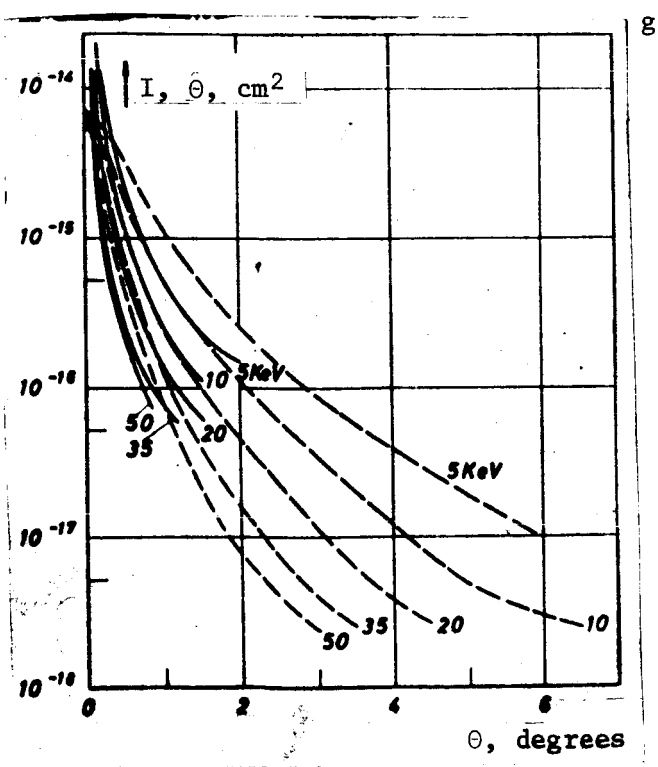

Figure 3. Differential Scattering Cross Sections for Electrons of Various Energy in N_2.

4.2 Inelastic Scattering

If the energy loss is greater than $(m_o/M)E$, then we are dealing with inelastic scattering. In this process, the electrons can ionize

the molecules, dissociate them, or bring about the excitation of discrete electrical levels. All processes are considered from the viewpoint of the inelastic differential scattering cross section $J_u(\vartheta)$, which was also calculated by Muntz and Marsden [13] on the basis of an approximation by Marton and Schiff, and is likewise plotted in Figure 3 with respect to ϑ. We see that $J_u(\vartheta)$ drops off rapidly with increasing ϑ, and is only greater than $J_{el}(\vartheta)$ for angles $\vartheta < 1°$.

The energy dependence can be calculated from the scattering formula of Mott and Massey [14]

$$Q_u(E, \Delta E) = \frac{64\,\pi^5 m_o^2 e_o^4}{(2\pi\, m_o v_e/h)^2 h^4} |z|^2 \ln \frac{2 m_o v_e^2}{\Delta E} \qquad (14)$$

and amounts to

$$Q_u \sim \frac{1}{E} \ln E \qquad (15)$$

The abbreviations used in equation (14) are as follows: m_o = electron mass, e_o = elementary charge, v_e = electron velocity, h = Planck's constant, ΔE = energy lost in the inelastic scattering process, and $|z|$ = matrix element for the transition which absorbs the energy ΔE. /19

In the proper manner, formulas (12) and (13) can also be applied to the case of inelastic scattering, if the subscript el is replaced by u. The density dn_e of the scattered electrons is given by dn'_e/v_e. Using equation (13), from equation (12) we obtain a differential equation for the decrease in electron density, in which we must insert the value for inelastic scattering (the minus sign designates the fact that it is a decrease):

$$\frac{dn_e}{n_e} = -N \cdot Q_u \cdot dy \qquad (16)$$

Inserting the initial electron density n_{eo}, we obtain:

$$\frac{n_e}{n_{eo}} = e^{-N \cdot Q_u \cdot y} \qquad (17)$$

Expression (17) now makes it possible to evaluate electron beam convergence if the values supplied by the wind tunnel are inserted for N and y. A desired ratio n_e/n_{eo} can be achieved by finding a suitable Q_u by varying the electron energy. On the other hand, for a predetermined ratio n_e/n_{eo} and a given electron

density, the maximum possible molecular density can be obtained.

4.3 Vibrational Temperature

In the case of inelastic scattering of electrons by nitrogen molecules, primarily the transition from the ground state $N_2\ X^1\Sigma_g^+$ to the ionized excited state $N_2^+\ B^2\Sigma_u^+$ is caused, which is converted by radiation to the ground state $N_2^+\ X^2\Sigma_g^+$ of the ionized nitrogen molecule (Figure 4). Figure 5 shows the spectrum of this transition. In addition to the most intensive line of the 0, 0 transition, additional lines can also be recognized, which come about through the superimposition of the electronic transition on the vibrational transitions.

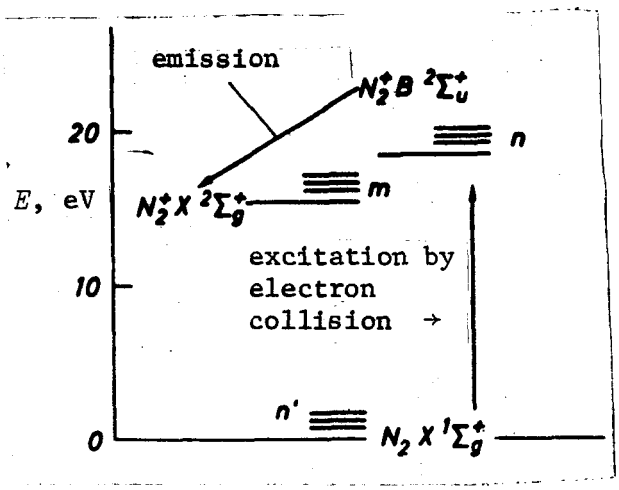

Figure 4. Diagram of the Transitions of the N_2 Molecules in Question.

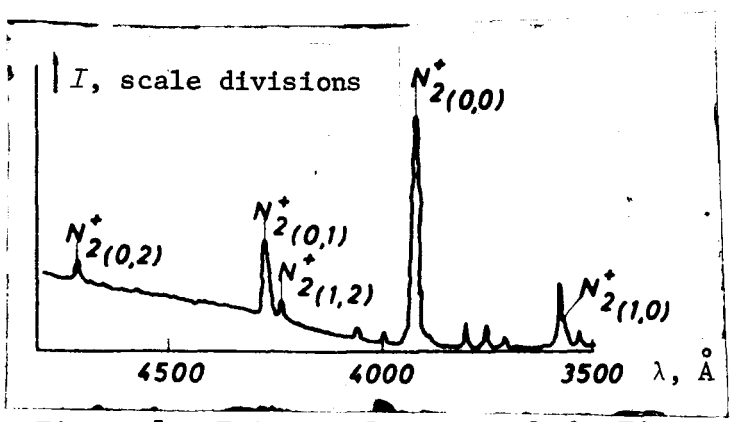

Figure 5. Emission Spectrum of the First Negative System of N_2 for the Case of Excitation by Electron Collision.

The theoretical prediction of the intensity of the vibrational transition as a function of the vibrational temperature T_V makes it possible to determine the temperature by measuring the intensities. In this process it is assumed that the gas-kinetic collisions do not disturb the excitation and radiation processes, that the wave functions for the electronic and the vibrational transition are separable, and that, finally, the occupation probability for the vibrational level is given by a Boltzmann distribution with the single parameter T_V. /20

According to [4], the emitted intensity for a transition n, m is given by

$$I_{nm} = N_n\, h c \nu_{nm} A_{nm}, \quad (18)$$

where N_n is the number of molecules which can make the transition n, m; h is Planck's constant; c is the speed of light; ν_{nm} is the wave number of the emitted light quanta; and A_{nm} is the Einstein transition probability for spontaneous transition.

The quantity A_{nm} is given by

$$A_{nm} = \frac{64\pi^4 \nu_{nm}}{3h} |R_{nm}|^2 \qquad (19)$$

The quantity $|R_{nm}|$ is the matrix element for the transition n, m, and can be provided in the wave-mechanical formulation according to the Frank-Condon principle by the function

$$|R_{nm}|^2 = \bar{R}_e^2 \left[\int \psi_v^n \psi_v^m d^3 r\right]^2 \qquad (20)$$

The quantity $\bar{R}_e$ in this case is the electrical transition element obtained over the intermolecular distance r traversed during the vibration. The second factor represents the overlap integral for the vibrational transition n, m. In order to determine the number N_n of excited states which can make the transition n, m, we have included the Einstein transition probability for an absorption which leads from the ground state n' to the excited state n. In this process, we must carry out a summation over all the possible states n':

$$N_n = \sum_{n'} \cdot N_{n'} \cdot B_{n\,n'} \cdot E_{n\,n'} \qquad (21)$$

The quantity $N_{n'}$ is the number of molecules in the ground state with the vibra- /21
tional quantum number n', which is provided by the assumed Boltzmann distribution

$$N_{n'} = \frac{N}{Z_V} e^{-G_o(n')\,hc/kT_V} \qquad (22)$$

The quantity N is the molecular density, Z_V is the state summation $Z_V = \sum_{n'} e^{-G_o(n')hc/kT_v}$, and $G_o(n')hc$ is the energy of the vibrational state n' above the ground state $n' = 0$. $E_{nn'}$ is the energy of the transition and is to be replaced by a mean energy E.

The transition probability $B_{nn'}$ is finally given once more by the Frank-Condon factor for absorption:

$$B_{n\,n'} = \frac{8\pi^3}{3h^2 c} |R_{n\,n'}|^2 = \frac{8\pi^3}{3h^2 c} \bar{R}_e^2 \left[\int \psi_v^n \psi_v^{n'} d^3 r\right]^2 . \qquad (23)$$

With

$$D = E\frac{N}{Z_V}\left(\frac{8\pi^3}{3h^2c}\right)\left(\frac{64\pi^4}{3h}\right) hc$$

for the intensity we obtain:

$$J_{nm} = D \cdot \nu_{nm}^4 \left|R_{nm}\right|^2 \sum_{n'} e^{-G_o(n')hc/kT_V} \cdot \left|R_{nn'}\right|^2 \qquad (24)$$

Let us now consider the intensity of the vibrational transitions 0,1 and 1,0 in the case of the electronic transition $N_2^+ \; B^2\Sigma_n^+ \rightarrow X^2\Sigma_g^+$ and let us form the ratio $J_{0,1}/J_{1,0}$:

$$\frac{J_{0,1}}{J_{1,0}} = \left(\frac{\nu_{0,1}}{\nu_{1,0}}\right)^4 \frac{\left|R_{0,1}\right|^2}{\left|R_{1,0}\right|^2} \frac{\sum_{n'}\left(e^{-G_o(n')\,hc/kT_V} \cdot \left|R_{0,n'}\right|^2\right)}{\sum_{n'}\left(e^{-G_o(n')\,hc/kT_V} \cdot \left|R_{1,n'}\right|^2\right)} \qquad (25)$$

The values for $|R_{0,1}|^2$, $|R_{1,0}|^2$, $|R_{0,n'}|^2$, and $|R_{1,n'}|^2$ are presented in tabular form and were given by Muntz [3]. The quantity $G_o(n')$ can be expressed by /22

$$G_o(n') \approx \omega_o n' - \omega_o x_o n'^2, \qquad (26)$$

where ω_o and x_o are molecular constants, and for $N_2 \; X^1\Sigma_g^+$ assume the values [4]

$$\omega_o \approx \omega_e = 2\,359{,}6 \text{ cm}^{-1}$$

and

$$\omega_o x_o \approx \omega_e x_e = 14{,}5 \text{ cm}^{-1}$$

For $T_V \rightarrow \infty$, for the ground state with $n' = 0$, we have the occupation probability 1. For other $n' = 1,2\ldots$ and T_V, the relative occupation probability can be calculated using an experimental law. In this manner, a theoretical description of the dependence of the intensity ratio on the vibrational temperature T_V is possible, as is shown in Figure 6.

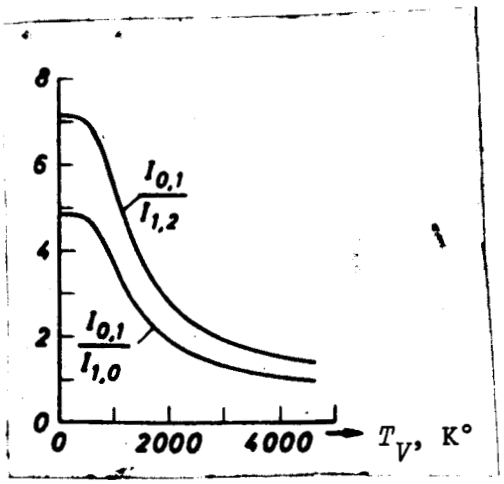

Figure 6. Ratio of the Band Intensities $J_{0,1}/J_{1,2}$ and $J_{0,1}/J_{1,0}$ as a Function of the Vibrational Temperature T_V.

Sebacher and Duckett [15] plotted the two intensity ratios, $J_{0,1}/J_{1,0}$ and $J_{0,1}/J_{1,2}$, against the vibrational temperature T_V. It can be seen that in the range from 500°K to 3,000°K, a sensitive change in the intensity ratio takes place with respect to temperatures. This is exactly the range through which the vibrational temperature passes during relaxation processes in expansion flow, if the maximal static temperature is T_0 = 3,000°K.

4.4 Rotational Temperature

In addition to the spectroscopic observation of the rotational fine structure of the $N_2^+ B^2\Sigma_n^+ \rightarrow X^2\Sigma_g^+$ transition, the electron beam method permits the determination of the rotational temperature T_R. Since the gas requires only 10 to 100 collisions in order for equilibrium to become established between translation and rotation, the rotational temperature T_R is a measure of the static temperature T in the measuring strip. Then the vibrational relaxation can be determined from the difference between the vibrational and the rotational temperatures, and the relaxation time can be thus calculated. /23

As a simplified representation of Sebacher and Duckett [15] shows, the intensity $J(K',T_R)$ of the rotational line can be described by

$$J(K', T_R) = [G]\, \nu^4\, K'\, e^{-B_{n'} K'(K'+1)hc/kT_R} \qquad (27)$$

The quantity $[G]$ is a weighting factor weakly dependent on T_R. K' is the rotational quantum number in the initial state $N_2^+ B^2\Sigma_n^+$, and $B_{n'}$ is a molecular constant which exhibits a weak dependence on the vibrational quantum number of the ground state $N_2\ X^1\Sigma_g^+$. The formula applies for the resolved R branch of the 0,0 transition and assumes this simple form, since the orbital angular momentum of the molecule is $\Lambda = 0$. A detailed derivation of formula (27) is found in the report by Muntz [3]. It was shown that the change in the intensity distribution by higher excited vibrational levels of the N_2 ground state up to 4,000°K is not significant, if an error up to *ca.* ±5% is permissible.

Figure 7 shows the rotational spectrum of the 0,0 band of the transition $N_2^+ B^2\Sigma_n^+ - X^2\Sigma_g^+$. There are two series of rotational lines which differ in

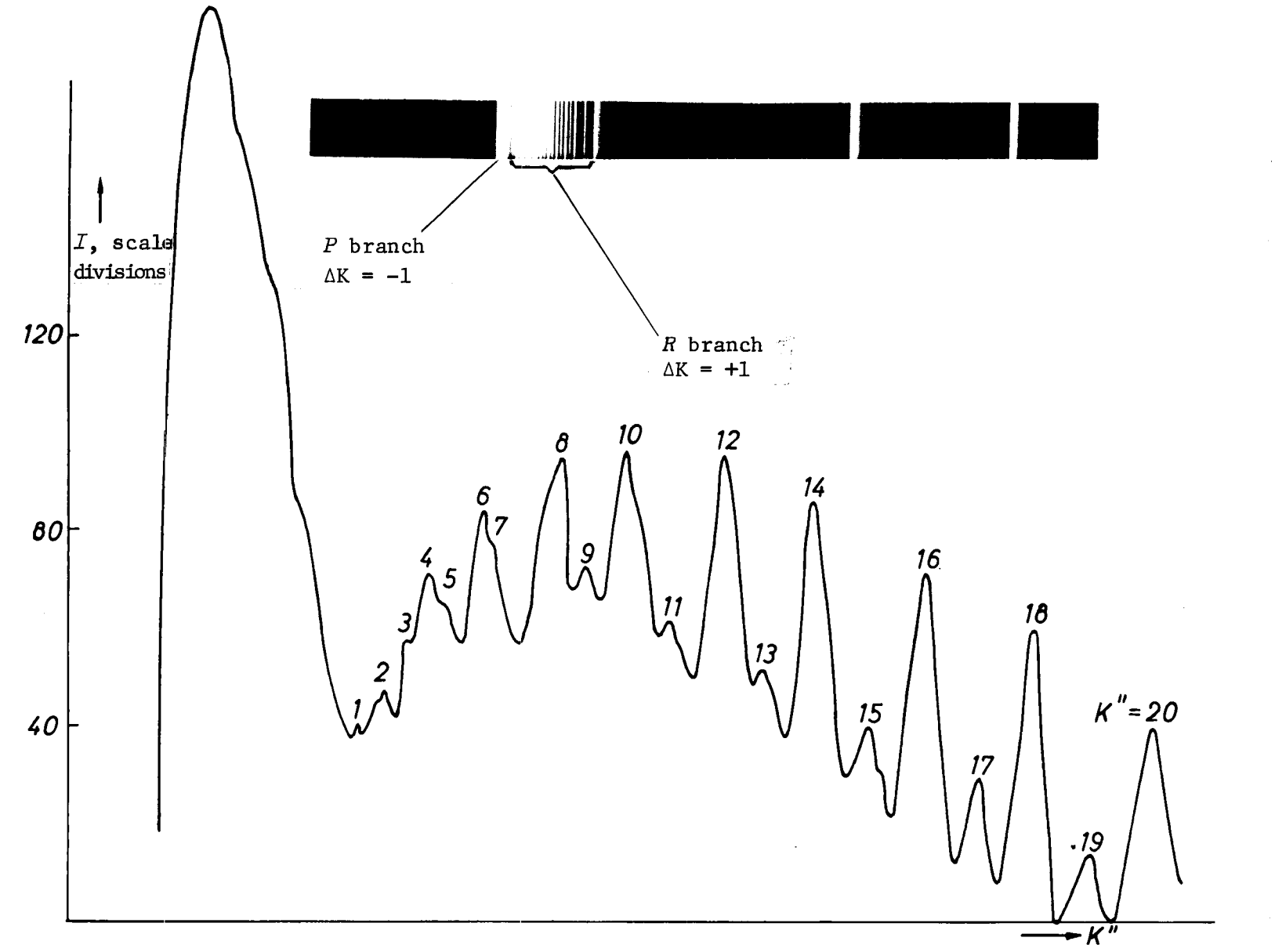

Figure 7. Rotational Spectrum of the 0,0 Band of the Transition $N_2^+ B^2\Sigma_g^+$.

intensity by the factor 2. The more intensive ones are applicable for even K'', and the others for odd K'', if K'' designates the rotational quantum number of the final state. According to formula (27), log $(J/[G]\nu^4 K')$ is plotted

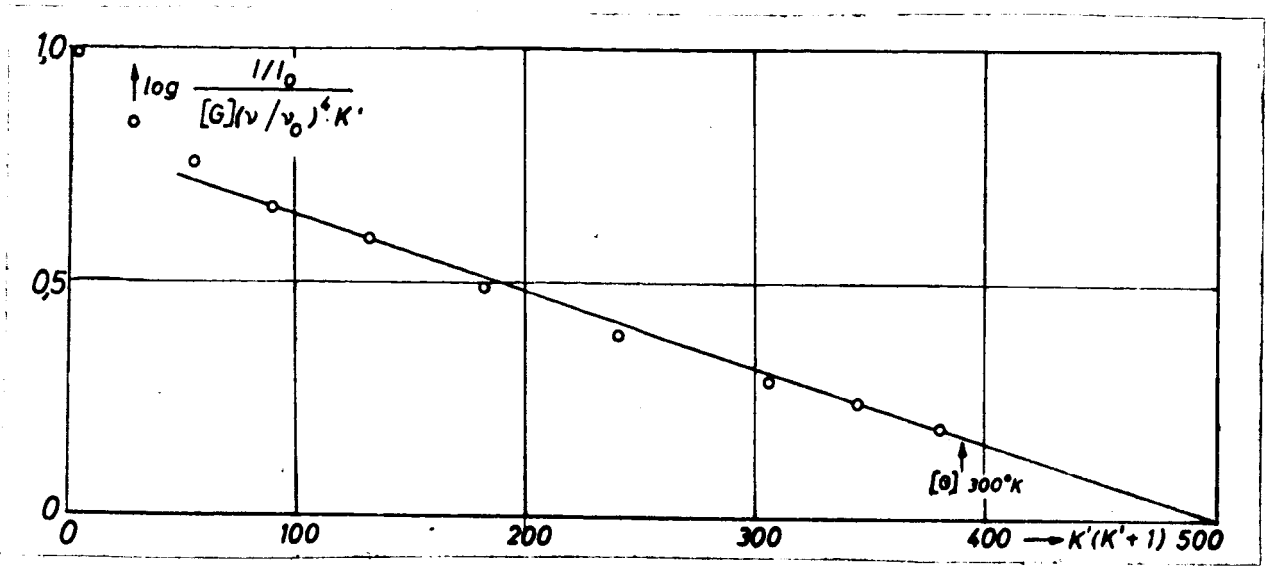

Figure 8. Graph of Log $\dfrac{J/J_0}{[G](\nu/\nu_0)^4 \times K'}$ Versus $K'(K' + 1)$ for Determining the Rotational Temperature.

against $K'(K' + 1)$ in Figure 8. The increase in the resulting straight line then yields the rotational temperature, T_R = 870°K.

4.5 Density

According to a simple treatment by Muntz [3], based on the equilibrium of the excitational levels $N_2^+ B^2\Sigma_n^+$ populated by electron collisions and depopulated by radiation and radiation-less transitions during molecular collisions, the intensity J of the electron excitation channel is given by

$$J = \frac{J'}{F} = \frac{N h c \nu_{nm}}{1 + \dfrac{2N\sigma^2\sqrt{4\pi RT}}{A_{nm}}} \qquad (28)$$

/24

The terms used in equation (28) signify the following: N = molecular density, ν_{nm} = the wave number of the transition, $N\sigma^2\sqrt{4\pi RT}$ = the gas-kinetic collision

number, A_{nm} = the Einstein transitional probability for the transition n, m, and F = the excitation function for the production of excited states.

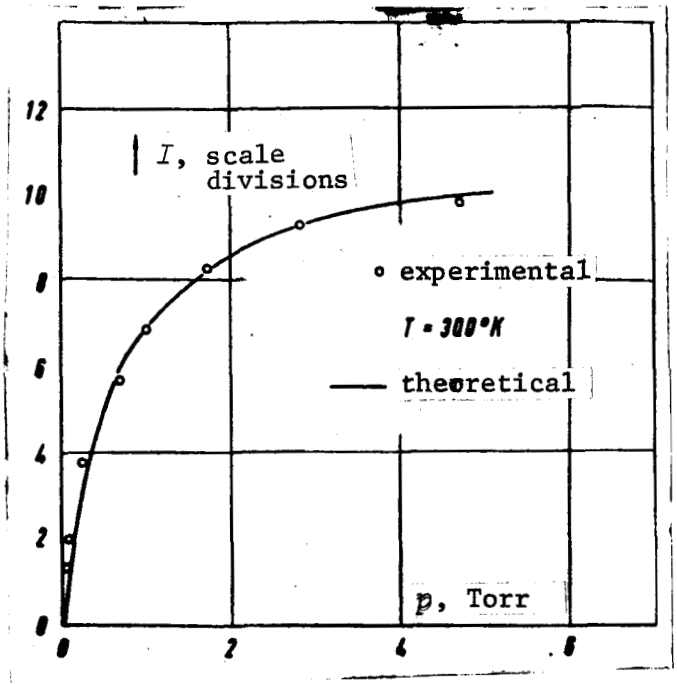

Figure 9. Dependence of the 0,0 Band Intensity on the Test Gas Pressure at T = 300°K.

The dependence of the intensity on the molecular density at room temperature has been plotted in Figure 9. The measured points lie quite well on the curve, which has been fitted to the measured points using the value $2\sigma^2\sqrt{4\pi RT}/A_{nm} = 6.8 \times 10^{-17}$. For sufficiently small densities, a linear dependence results. This is the case when

$$2n\sigma^2\sqrt{4\pi RT}/A_{nm} \ll 1 \quad . \quad (29)$$

At room temperature, a deviation of 1% is to be expected at $N = 1.47 \times \times 10^{14}$ molecules/cm^3 or a pressure of 4×10^{-3} Torr.

In the case of density measurements in the measuring area of the hypersonic wind tunnel, a static temperature $T_T \approx T_R \approx 50$°K must be used, so that the left-hand side of (29) becomes even smaller. Then if we consider the temperature dependence of σ^2, the left-hand side becomes still smaller. Harbour and Lewis [12] estimate that σ^2 changes in proportion to $\sqrt{RT}/\eta(T)$, where $\eta(T)$ is the viscosity of the gas. But this can only be an estimation, and the actual conditions are described by a complicated law [16].

Expression (28) must be considered still further if we imagine that the vibrational temperature in the expansion flow is not in equilibrium with T_R. In the boundary layer and in collisions, T_V will assume other values than in undisturbed nuclear flow. Thus, the number of excited states is also different. This state of affairs will first be taken into consideration by computing the /25 excitation function F as a function of the vibrational temperature T_V, i.e., $F = F(T_V)$, and thus, for the intensity, we have the formula

$$J = F(T_V)\frac{n\,hc\,\nu_{nm}}{1 + \frac{2n\sigma^2\sqrt{4\pi RT}}{A_{nm}}} \quad (30)$$

More precise investigation will provide the quantitative relationships.

5. Apparatus

The entire apparatus is schematically represented in Figure 10. The electrons are emitted in a chamber evacuated to 10^{-4} Torr by a hot cathode and accelerated to the desired energy between 0 and 60 KeV. They pass through a system of diaphragms and pressure stages and the measuring chamber of the hypersonic wind tunnel, and are received in a Faraday collector. The anode current

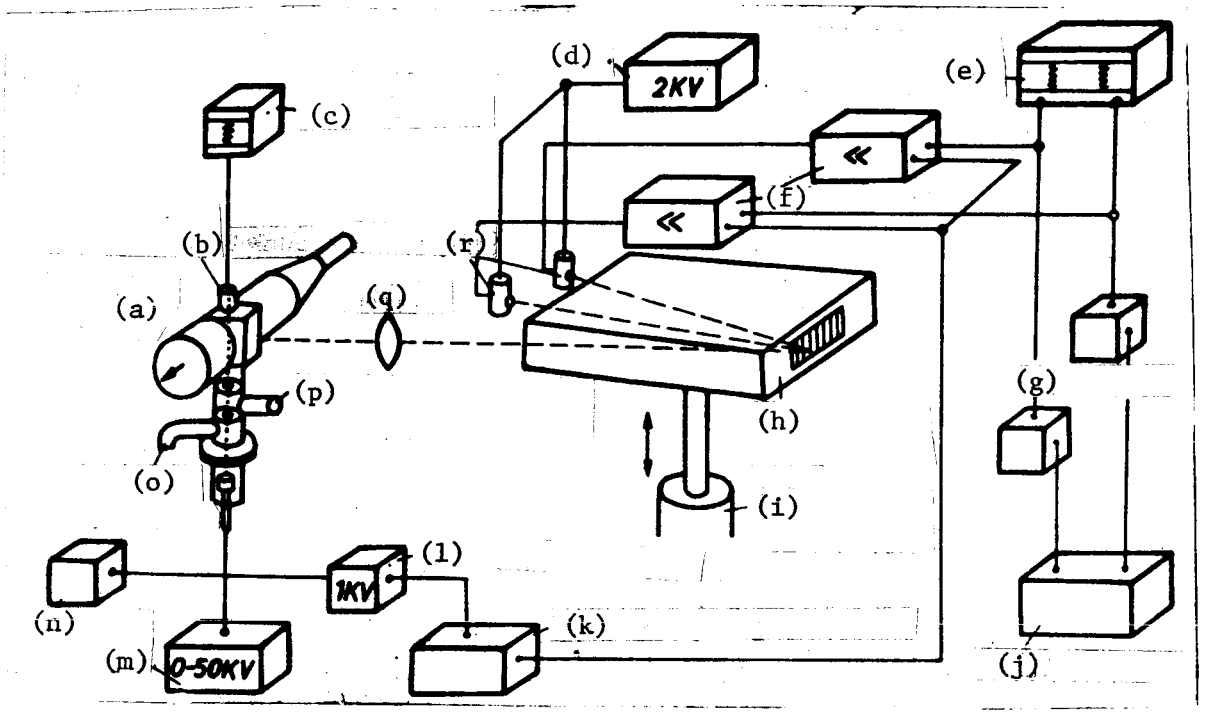

Figure 10. Overall Block Circuit Diagram of the Apparatus. Key: (a) hypersonic wind tunnel; (b) Faraday collector; (c) recorder; (d) multiplier voltage; (e) two-channel recorder; (f) lock-in multiplier; (g) digital voltmeter; (h) lattice spectrograph; (i) vertical adjustment; (j) printout; (k) pulsed voltage; (l) Wehnelt voltage; (m) high-voltage anode; (n) hot voltage; (o) diffusion pump, 10^{-4} Torr; (p) diffusion pump, 10^{-2} Torr; (q) lens; (r) multiplier.

can be measured with a recorder. The nitrogen molecules produced by electron collisions form a glowing area about 1 mm in diameter and the image of this line can be focused on the slit of a spectrograph by a quartz lens with a focal length of f = 15 cm.

5.1 The Electron Gun

Figure 11 shows the construction of the electron gun and the measuring portion of the wind tunnel.

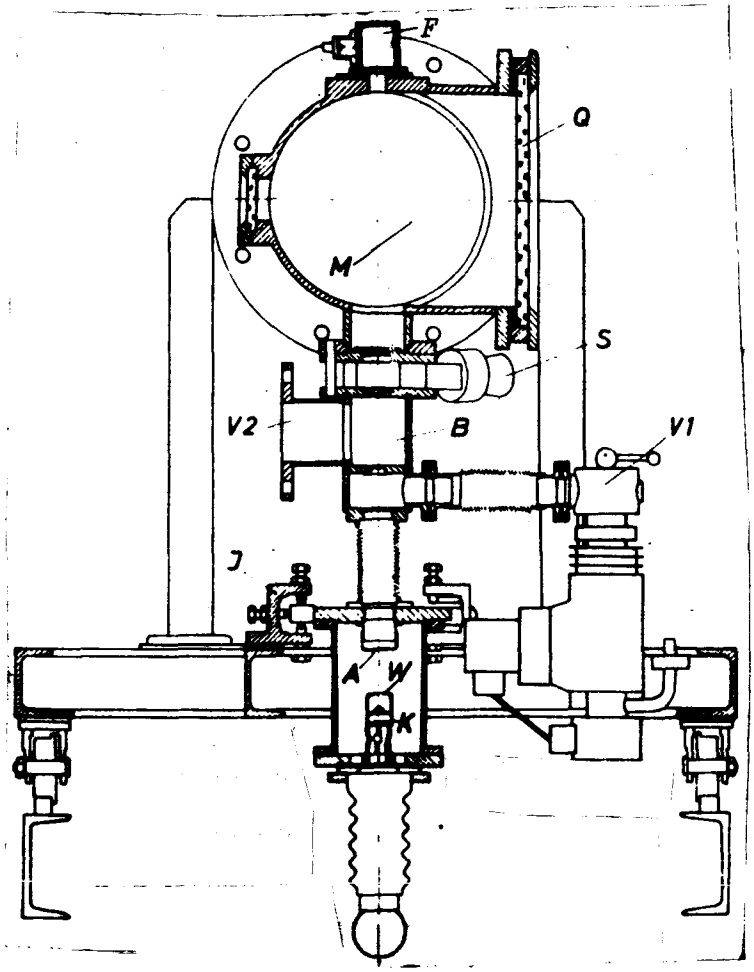

Figure 11. Sectional Diagram of the Electron Gun and Measuring Chamber. *A* = Anode; *B* = Diaphragm Chamber; *F* = Faraday Collector; *J* = Adjustment; *K* = Cathode; *M* = Measuring Area; *Q* = Quartz Glass Window; *S* = Slide; *V1*, *V2* = Connections to Vacuum Pump; *W* = Wehnelt Cylinder.

The electron production system is taken from the EM-8 electron microscope from Zeiss, Oberkochen. It is fastened to the floor of a chamber which is evacuated to less than 10^{-4} Torr by way of two spring steel bellows, using a DO-30L diffusion pump from Leybold, Cologn. The electron beam emerges from the hairpin cathode (*K*) of the electron production system and is accelerated by the high voltage applied to the anode (*A*) to the desired energy between 0 and 60 KeV. The anode, together with the Wehnelt /26 cylinder (*W*), forms an electrical lens which focuses the electron beam on a distant point. A mechanical adjustment (*J*) can be made by a three-point fastening of the upper chamber roof. The electron beam passes through a diaphragm chamber (*B*) with 1-mm borings, which is evacuated by a diffusion pump at a removal rate of 350 ℓ/sec. A slide (*S*) serves to separate the entire system from the wind tunnel and to evacuate it before an experiment. The measuring area (*M*) is connected to the slide. The Faraday collector (*F*), which is electrically insulated from the tunnel, lies on the opposite side. On the right-hand side, the recess with the quartz-glass window (*Q*) can be seen; it was furnished by Spindler and Hoyer, Göttingen. This provides the opportunity for observing the entire diameter of the measuring strip and has a maximal width of 80 mm. If this large slit width should cause any disturbance to the flow, its size can be reduced to 40 mm.

The measuring chamber is fastened by beams to a wagon which can be moved into the tunnel (1).

5.2 Voltage Supply of the Electron Gun

An instrument from Sorenson, South Norwalk, USA, is used to produce the high voltage. This is the Model 1061, which provides 0-6 kV at a maximum of 10 mA and has a 1.5% hum. The positive voltage is ground potential.

The hot voltage is taken from a transformer whose secondary winding is insulated from the ground potential in accordance with the high voltage. It provides 6.3 V and a maximum of 20 A.

The Wehnelt voltage is provided by an 800-V direct-current instrument which is fed from the hot transformer. As can be seen in Figure 12, the 6.3 volts are first transformed to 400 volts, rectified in a doubler switch, and stabilized in a stabilizing circuit. The potentiometer which can be applied above each /27 of the stabilizer tubes permits the voltage of each to be adjusted between 0 and 800 volts. Finally, a pulsed voltage can be superimposed on the Wehnelt voltage, so that a pulsed electron beam is available. The details can be seen in the circuit diagram, Figure 13.

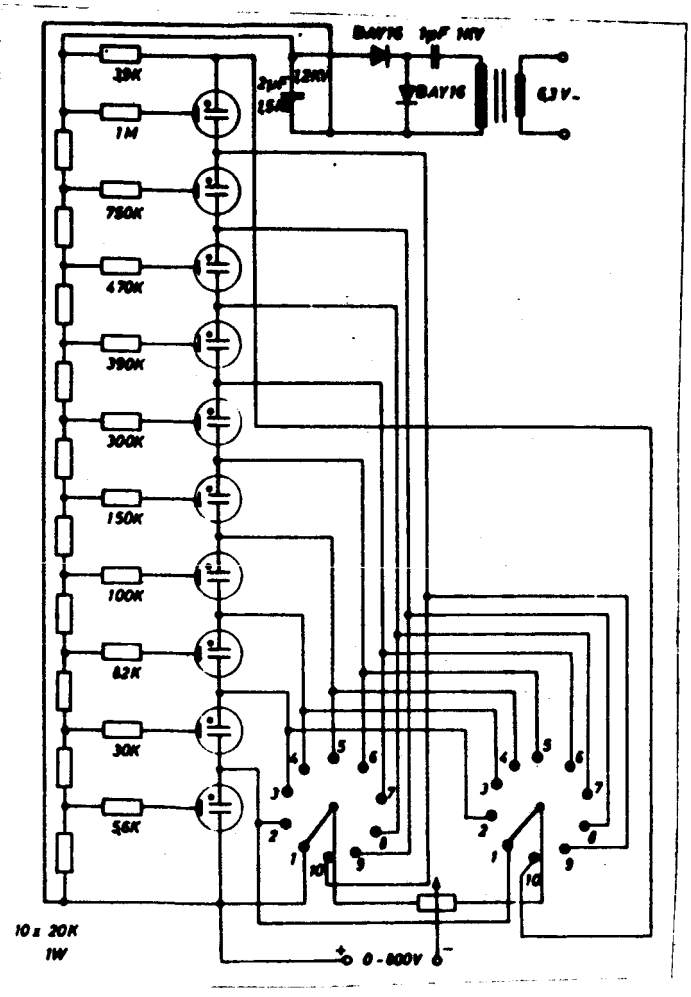

Figure 12. Circuit Diagram of the 800-Volt Voltage Supply.

5.3 Spectrograph with Multiplier

For the spectral analysis, a 1.5-m lattice spectrograph 33-83-01-11 from Bausch and Lomb, Rochester, N.Y., USA, is used. It operates in the first order from 3,700 to 7,400 Å with a linear dispersion of 15 Å/mm, and in the second order from 1,850 to 3,700 Å with a linear dispersion of 7.5 Å/mm. The wavelength of the flame is 3,500 Å. In the second order, a theoretical resolution capability of $\lambda/\Delta\lambda$ = 70,000 is achieved. The theoretical light intensity is about 1/27.5.

While monochromators have the advantage of greater light intensity, the spectrograph has the advantage of making the entire spectrum available at the same time.

Since the intensity ratio of two lines is used for determining the temperature, the corresponding positions in the spectrum are simultaneously sought

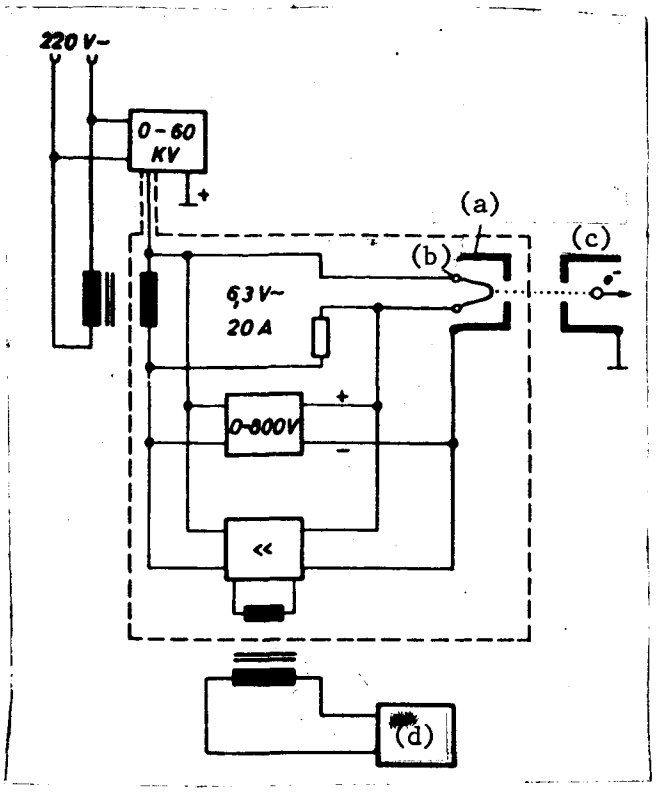

Figure 13. Voltage Supply of the Electron Gun. Key: (a) Wehnelt cylinder; (b) cathode; (c) anode; (d) pulse generator.

by two multipliers. The favorable arrangement of the lattice and the resulting positions of the first and second order permit the introduction of two multipliers side by side. They are fastened to a multiplier table placed next to the spectrograph. One motor-driven multiplier can traverse the entire spectrum. The second can be fixed at any desired position.

The multiplier used was RCA type 1-P28. It has an S5 characteristic and a quartz-glass housing. The entire spectrum lies within the 70% limits. The high voltage for the multiplier is provided by the PE-4839 apparatus from Philips, Hamburg. At a maximum current of 10 mA, 200 to 2,000 volts can be taken off. The stability is < 0.015% and the noise voltage is < 10 mV.

5.4 Recording /28

The output signals of the multipliers, which also pulse because of the pulsed electron beam, are fed into a lock-in amplifier. This amplifier is constructed according to the circuit diagram shown in Figure 14. The pulsed voltage of the pulse apparatus is fed into the amplifier as well as into the electron gun, so that an in-phase amplification is achieved: during one impulse, the multiplier delivers signal plus noise, and during the pause between two pulses, the multiplier delivers only the noise. A suitable setup in the amplifier forms the difference between the two contributions, so that finally only the signal is indicated. The signal-to-noise ratio can be kept down to 0.2:1 with an amplifier of this type.

The output voltage of the lock-in amplifier is fed into a two-channel recorder or to two digital voltmeters with printouts. The vibrational temperature can be determined from the ratio of the measured intensities, after suitable corrections, and the density in the measuring strip can be determined from the intensity of a single line, after suitable calibration. The sensitivity of this arrangement makes it possible to vary certain parameters during the wind tunnel experiment, such as the coordinates of the measuring strip, the static pressure or the static temperature, and then to record the changes in the intensities under consideration. In addition, this method makes it possible to carry out measurements in scattered light and daylight, which would otherwise be disturbing.

Lock-in Amplifier, Diagram No. 313

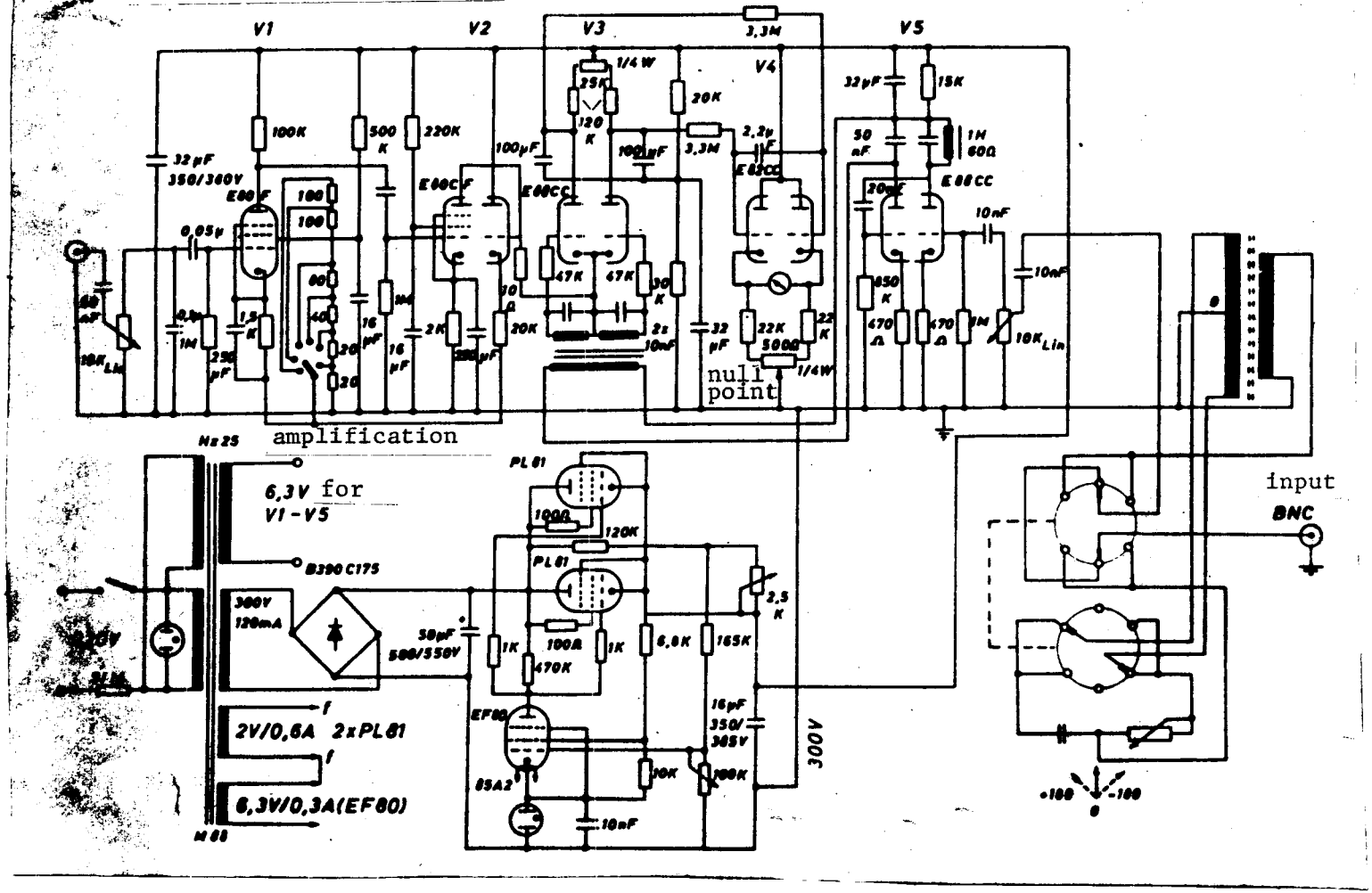

Figure 14. Circuit Diagram of the Lock-In Amplifier.

5.5 Corrections

The results which are measured according to the process just described must still be corrected from the viewpoint of spectral permeability and sensitivity of detection. In addition, we must also consider the fact that in measuring the intensities of the 1,0 and the 0,1 bands, the spectrograph is used in two different orders. The linearity of the amplifier must likewise be guaranteed.

To be sure, especially in the case of the multiplier, the sensitivity curve provided along with the instrument by the manufacturer could be used, but this curve is not very precise and therefore was not used. /29

One method for determining the spectral corrections consists in measuring the emission of a tungsten-band lamp in dependence on the wavelength and comparing it with the theoretical predictions obtained from the Planck radiation formula. Unfortunately, the tungsten-band lamp does not correspond very well to the properties of a black-body emitter. Therefore, this method was not used.

It is simpler to excite nitrogen at a known equilibrium temperature by electron collisions, measure the intensity ratios, and compare them with the theoretical values. Then, in a simple manner, the deviations provide the correction factors.

6. Measurement Protocol

First, the measurement of the rotational and vibrational temperatures and the density in the measuring area of the hypersonic wind tunnel will be used to determine the state of the test gas. The results will be compared with the calculations of Koppenwallner [2]. In addition, the calculations of Wuest [17] will be experimentally retested.

In a similar manner, as in the case of Harbour and Lewis [12], we will measure the density distributions on models and supplement them with temperature distribution measurements.

Finally, we intend to investigate the vibrational relaxations in the wakes of various models surrounded by flow paths.

7. Summary /30

Various methods for determining the vibrational temperature were studied with respect to their applicability in the hypersonic wind tunnel of the AVA at Göttingen. The results showed that, in general, the common methods were not applicable because of the special conditions in an expansion flow.

The sodium line reversal method is not possible since the loss of excited Na atoms by radiation is too great. The ultraviolet absorption method necessitates investigations in the far UV, which are very difficult.

Methods which use the ionizability of a gas cannot be applied because of the slight monochromaticity of the electrons and the destruction caused by the high velocity of the gas.

Raman spectroscopy cannot be carried out at such small gas densities.

In all the procedures mentioned above, the volume which is measured is so large that the spatial resolution is poor. Measurements on models are only conceivable in special cases.

The electron beam method does not have the disadvantages mentioned above. It permits good spatial resolution, so that measurements on models are possible. The theory of this method is described in detail in Section 4, based on reports by Muntz [3] and Herzberg [4].

Thus, it is evident that in addition to the local vibrational temperature, we can also measure the local rotational temperature and the local density. The vibrational temperature results in this method from the ratio of two band intensities. It can be theoretically predicted as a function of temperature. The rotational temperature is taken from the intensity distribution of the rotational spectrum. The density can be read from the intensity of a single band following suitable calibration.

The range of linearity for density measurements depends on the density and on the static temperature [3], [12]. The reasons are presented for the fact /31 that a dependence on the vibrational temperature must also be considered if this temperature is greater than 800°K, as in the case of an expansion flow with vibrational relaxations. The construction of the apparatus is described in Section 5. Since the spectrograph which was selected is able to measure the intensities of two bands at the same time, the vibrational temperature can be determined from the ratio of the intensities following suitable correction, and the density can be read from the intensity of a single band following suitable calibration. The very sensitive detection apparatus, which consists of photomultipliers and subsequent lock-in amplifiers in connection with a pulsed electron beam, makes it possible to measure vibrational temperature and density continuously as a function of position, static temperature, or static pressure, even in the presence of interfering light. The rotational temperature can be obtained from pictures of the rotational spectrum by permitting one multiplier to pass through the spectrum.

The correction factors necessitated by the apparatus are obtained by measuring the vibrational and rotational temperatures and density of the test gas under known conditions.

REFERENCES /32

1. Koppenwallner, G.: Experimental technique with rarified gases. In: *4. Lehrgang für Raumfahrttechnik. (Fourth Lecture Series on Space Travel Technology.)* Göttingen, 1965.
2. Vas, I. E. and G. Koppenwallner: *The Princeton University High Pressure Hypersonic Nitrogen Tunnel N-3.* Princeton University Dept. of Aerospace

and Mech. Sci., Report No. 690, 1964.

3. Muntz, E. P.: *Measurement of Rotational Temperature and Molecule Concentration in Nonradiating Flows of Low Density Nitrogen.* University of Toronto, Institute of Aerophysics (UTIA), Report No. 71, 1961.
4. Herzberg, G.: *Molecular Spectra and Molecular Structure, Vol. 1.* D. van Nostrand Company, Princeton, N.J., 1965.
5. Hurle, I. R., A. L. Russo and I. Gordon Hall: *Experimental Studies of Vibrational and Dissociative Nonequilibrium in Expanded Gas Flows.* AIAA Conference on Physics of Entry into Planetary Atmospheres, Massachusetts Institute of Technology, 1963.
6. Koppenwallner, G.: *Der Hypersonische Vakuumwindkanal der Aerodynamischen Versuchsanstalt Göttingen -- Betriebsverhalten und erste Ergebnisse über reale Gaseffekte in Düsenströmungen. (The Hypersonic Vacuum Wind Tunnel of the Aerodynamic Research Institute at Göttingen -- Performance in Operation and First Results Concerning Real Gas Effects in Nozzle Flows.)* DGRR/WGLR Annual Meeting in Bad Godesberg, No. 66-113, 1966; AVA Report 66 A 42, 1966.
7. Gaydon, A. G. and I. R. Hurle: *The Shock Tube in High-Temperature Chemical Physics.* Chapman and Hall, Ltd., London, 1963.
8. Gaydon, A. G. and H. G. Wolfhard: *Flames, their Structure, Radiation and Temperature.* Chapman and Hall, Ltd., London, 1960.
9. Camac, M.: O_2 vibrational relaxation in oxygen-argon mixtures. *J. Chem. Phys.*, Vol. 34, p. 448, 1961.
10. Pohl, R. W.: *Optik und Atomphysik. (Optics and Atomic Physics.)* Springer/33 Verlag, Göttingen, 1958.
11. Brunnee, C. and H. Voshage: *Massenspektrometrie. (Mass Spectrometry.)* K. Thiemig Verlag KG, Münich, 1965.
12. Harbour, P. J. and J. H. Lewis: *Preliminary Measurements of the Hypersonic Rarefied Flow Field on a Sharp Flat Plate Using an Electron Beam Probe.* Fifth International Symposium on Rarefied Gas Dynamics, Book of Abstracts, Oxford, 1966, p. 173.
13. Muntz, E. P. and D. J. Marsden: Electron excitation applied to the experimental investigation of rarefied gas flows. In: *Rarefied Gas Dynamics. Proceedings of the 3rd International Symposium on Rarefied Gas Dynamics, Paris, 1962. Vol. 2.* Academic Press, New York, 1963, pp. 495-526.
14. Mott, N. F. and H. S. W. Massey: *The Theory of Atomic Collision.* Oxford Univ. Press (Clarendon), London and New York, 1952.
15. Sebacher, D. I. and R. J. Duckett: *A Spectrographic Analysis of a 1-Foot Hypersonic-Arc-Tunnel Airstream Using an Electron Beam Probe.* NASA TR R-214, 1964.
16. Liepmann, H. W. and A. Roshko: *Elements of Gas Dynamics.* Galcit Aeron. Series, J. Wiley and Sons, Inc., New York and London, 1960.
17. Wuest, W.: *Hypersonic Flow Through Nozzles with Vibrational Relaxation.* AVA Report 66 A 40, 1966.

FRANK C. FARNHAM COMPANY, INC.
133 South 36th Street
Philadelphia, Penna. 19104
Translated by Linda R. Henson
NASW-1497